

12 N64-25775

CODE 1

CAT. 29

NASA CR-56972

12p. Technical Report No. 32-629

Convective Heat Transfer in Planetary Atmospheres

Daniel J. Collins

jpl

JET PROPULSION LABORATORY
CALIFORNIA INSTITUTE OF TECHNOLOGY
PASADENA, CALIFORNIA

July 1, 1964

OTS PRICE

XEROX

\$ 1.60 ph

MICROFILM

\$ _____

ERRATA dated 19 Oct 1964 inserted

Technical Report No. 32-629

Convective Heat Transfer in Planetary Atmospheres

Daniel J. Collins


Bain Dayman, Jr., Chief
Aerodynamics Facilities Section

**JET PROPULSION LABORATORY
CALIFORNIA INSTITUTE OF TECHNOLOGY
PASADENA, CALIFORNIA**

July 1, 1964

Copyright © 1964
Jet Propulsion Laboratory
California Institute of Technology

Prepared Under Contract No. NAS 7-100
National Aeronautics & Space Administration

CONTENTS

I. Introduction	1
II. Experimental Measurements	2
III. Results	4
IV. Conclusions	7
Nomenclature	7
References	8
Table 1. Property values of gauge materials	2

FIGURES

1. Typical heat transfer model	2
2. Calorimeter circuit	3
3. Calorimeter trace	3
4. Monitoring photocell	3
5. Photographs of shock	3
6. Raster output	4
7. Stagnation point heat transfer measurements	5
8. Stagnation point heat transfer 9 % CO ₂ , 90 % N ₂ and 1 % A	5
9. Stagnation point heat transfer 100 % CO ₂	5
10. Stagnation point heat transfer 65 % CO ₂ and 35 % A	6
11. Effect of different gauge materials on stagnation point heat transfer	6

ABSTRACT

25775

Convective heat transfer rates for three model planetary atmospheres have been obtained. These atmospheres are characteristic of those about the planets Mars and Venus. Atmospheres consisting of nitrogen and carbon dioxide gave heat transfer rates similar to that of air. The presence of argon materially increased the heat transfer rate.

The effects of different gauge materials on the convective heat transfer were also measured. No major differences were found for the experimental conditions studied.

author

I. INTRODUCTION

An extensive program of convective heat transfer measurements in simulated planetary atmospheres has been completed at the Jet Propulsion Laboratory (JPL). The purpose of this series of investigations was to describe the effects due to atmospheric composition in convective heat transfer to planetary probes entering the atmospheres of the near planets.

Since the present knowledge of the atmospheric compositions of Mars and Venus is slight, three different simulated atmospheres were investigated. Model Atmos-

phere I consisted of 9% CO_2 , 90% N_2 and 1% A. This is presently considered to be the most likely composition of the Venus atmosphere. Since the atmosphere of Mars is believed to contain a large percentage of carbon dioxide, the second planetary atmospheric model was taken to be 100% CO_2 . Comparisons are given with experimental measurements of other laboratories for these two atmospheres.

Recent studies (Ref. 1) indicate that the Mars atmosphere could contain 35% argon. Therefore, the third

atmospheric model consisted of 35% A and 65% CO₂. It is believed that this is the first report dealing with argon and carbon dioxide atmospheres.

As part of the basic investigations, a study was also made of the effects of different gauge materials on the measured convective heat transfer. For Model Atmos-

phere I, tests were made with both gold and nickel calorimeters in addition to the standard measurements made with platinum calorimeters. All measurements were made in the JPL 6-in. hypervelocity shock tube which is fully described in Ref. 2. A range of shock speeds from approximately 17,000 ft/sec to 32,000 ft/sec was covered. Initial pressure ranged from 0.25 mm Hg to 1.00 mm Hg. Typical test times were from 10 to 25 μ sec.

II. EXPERIMENTAL MEASUREMENTS

The experimental technique for obtaining convective heat transfer measurements has been extensively described by Rose (Ref. 3). Essentially, the calorimeter gauge is a heat sensitive element thick enough so that all transferred energy remains in the gauge. Figure 1 shows the 1-in. D hemispherical model used in obtaining the data. The platinum calorimeter has a thickness of 0.0010 in.

The heat transfer rate is given by

$$\dot{q} = \frac{d}{dt} \left\{ \frac{\rho c l}{\alpha R_o} R \right\}$$

or in terms of measured quantities with a constant gauge current,

$$\dot{q} = \left\{ \frac{\rho c l}{\alpha R_o I_o} \right\} \frac{dE}{dt}$$

The platinum properties have been determined from values specified by the manufacturer for high purity platinum. The manufacturer's values are in agreement with the National Bureau of Standards (NBS) values. The temperature coefficient of electrical resistance has been determined independently. Table 1 lists the property values for platinum as well as for nickel and gold calorimeters. The property values for nickel and gold were obtained from the Handbook of Physics and the NBS. The specific heat of nickel was verified by an independent laboratory.

The basic calorimeter circuit is shown in Fig. 2. All elements of the circuit are precisely balanced in order to

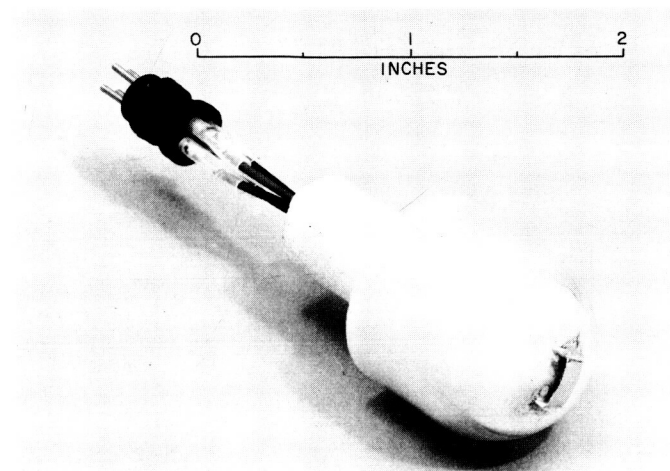


Fig. 1. Typical heat transfer model

Table 1. Property values of gauge materials

Property value	Platinum	Gold	Nickel
Density, g/cm ³	21.45	19.3	8.9
Specific heat, cal/°C/g	0.0320	0.0317	0.1095
Temperature coefficient of resistivity	3.92×10^{-3}	3.42×10^{-3}	6.0×10^{-3}
Thickness, in.	0.0010	0.0020	0.0020

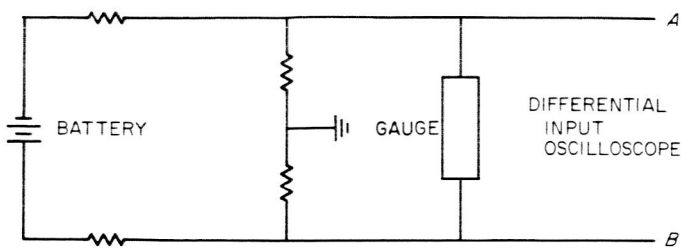


Fig. 2. Calorimeter circuit

obtain as clean a signal as possible. The starting transient on the calorimeter trace is minimized if the circuit as well as the preamplifier is carefully balanced. A typical calorimeter trace is shown in Fig. 3. The initial disturbance at the beginning of the trace is due to a capacitance effect between the shock wave and the gauge. The arrival of the contact surface is indicated by the slight notch at the end of the trace. At higher shock speeds, the gauge output oscillates violently after the arrival of the contact

surface. The linear slope of the calorimeter trace is in itself an indication of a good slug of test gas. Verification of a good test slug is, of course, a very necessary part of any hypervelocity experimental measurement. A further check is obtained on the quality of the test gas by means of a monitoring photocell which is collimated in front of the model. At the higher shock speeds the turbulent contact surface can swallow the test slug. Figure 4 is the monitoring photocell output for the same run as that indicated by the calorimeter trace. A poor test slug would be indicated by a sloping line on the trace. The dip in the trace at the beginning of the monitoring photocell indicates that flow over the model becomes established in approximately 3 μsec .

In the original development of the hypervelocity shock tube, extensive pictures were taken of the traveling shock in order, as explained in Ref. 2 to verify the existence of a plane shock. Several pictures of the shock before the model and of the established flow on the model were taken by an image converter camera. A typical set of photographs is shown in Fig. 5. All the diagnostic methods (straight calorimeter trace, flat monitoring photocell output, and photographs of the shock) correlated well with each other. Thus, a good calorimeter trace was obtained when good test time was indicated by the monitoring photocell. If the photograph indicated a tilted shock, the calorimeter trace was erratic.

The shock speed was obtained from 3 pairs of photocell pickups located in front of the model. The photocell

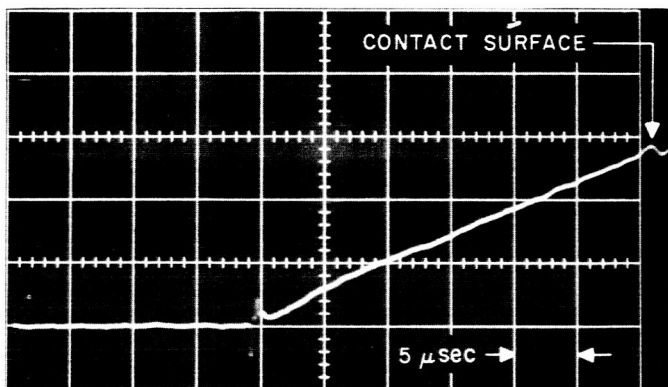


Fig. 3. Calorimeter trace

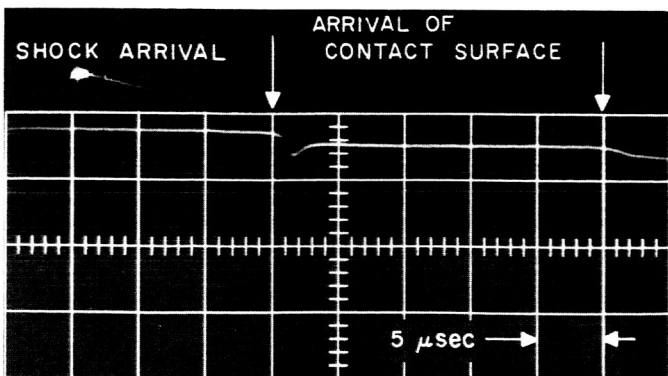


Fig. 4. Monitoring photocell

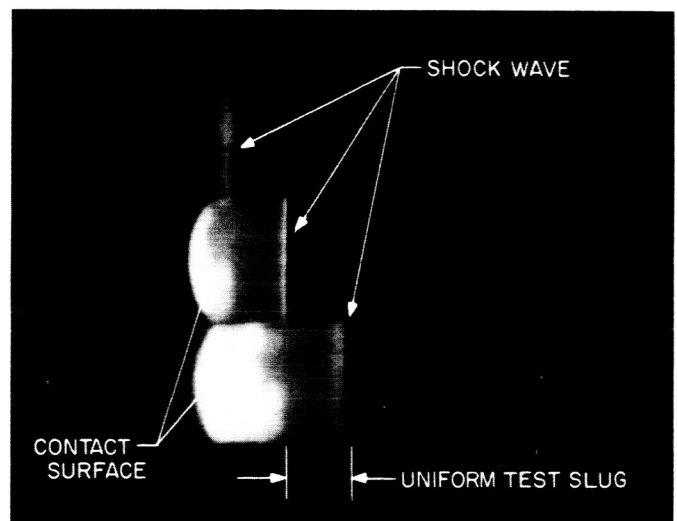


Fig. 5. Photographs of shock

output was fed into a raster display. The raster output is shown in Fig. 6. The time markers (dots) are $10\ \mu\text{sec}$ apart. An indication of the arrival of the shock front at each of the six photocells can be seen on the trace. The shock speed at the test station was obtained by extrapolating the measured shock speeds to the test point.

The initial pressure in the shock tube was measured to an accuracy of $\pm 5\mu$ by means of a system designed at JPL. This system is fully described in Ref. 2. Initial pressures ranged from 0.25 mm Hg to 1.00 mm Hg.

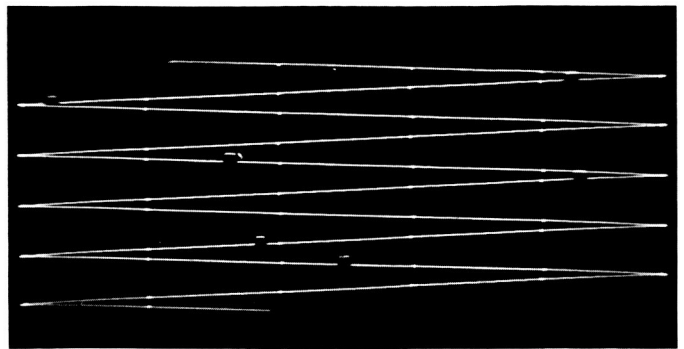


Fig. 6. Raster output

III. RESULTS

The experimental results for Model Atmosphere I (9% CO_2 , 90% N_2 and 1% A) are given in Figs. 7 and 8. The comparison of experimental measurement of the model atmosphere having only 9% CO_2 with that of AVCO air data (Ref. 4) appears in Fig. 7.

In this particular model atmosphere, the convective heat transfer does not differ greatly from that of air. The data are correlated with respect to the square root of the model radius. No correction for radiative heat transfer has been made to the data, since it would amount to less than 10%.

In Fig. 8, a comparison is made with General Electric (GE) data (Ref. 5) for essentially the same atmosphere (9% CO_2 , 91% N_2). The data have been further correlated by dividing by the square root of the stagnation pressure. Excellent agreement is indicated by the data.

The experimental results for Model Atmosphere II (100% CO_2) are given in Fig. 9. A comparison is made with the JPL Model I data. The general trend of the 100% CO_2 data is of the order of 10% higher than the 9% CO_2 data. A further comparison is given with data presented by Nerem, Morgan, and Grabler (Ref. 6).

The experimental results for Model Atmosphere III (65% CO_2 , 35% A) are presented in Fig. 10. Again, a comparison is made with the results for Model Atmosphere I (9% CO_2 , 90% N_2 and 1% A). A large increase in the convective heat transfer over that of the CO_2 -air mixture is indicated. At 25,000 ft/sec, which is approximately the Martian entry velocity, there is approximately a two fold increase in the convective heat transfer.

Figure 11 shows the effects of different gauge materials (Ref. 7). The data in Fig. 11 indicate no major difference in the measured heat transfer rate due to gauge material for the test conditions investigated.

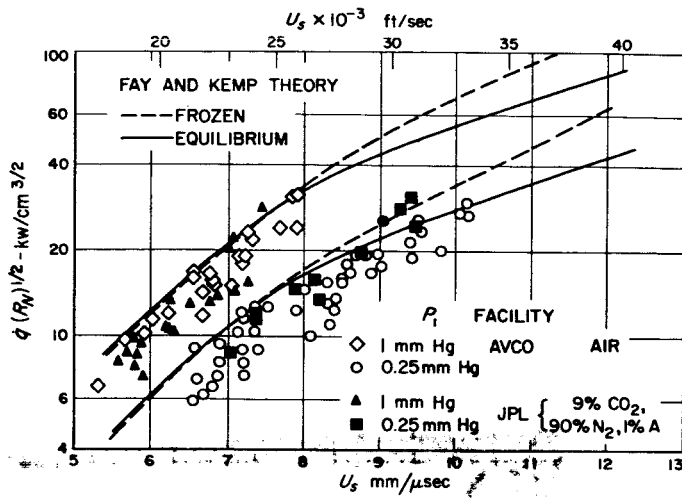


Fig. 7. Stagnation point heat transfer measurements

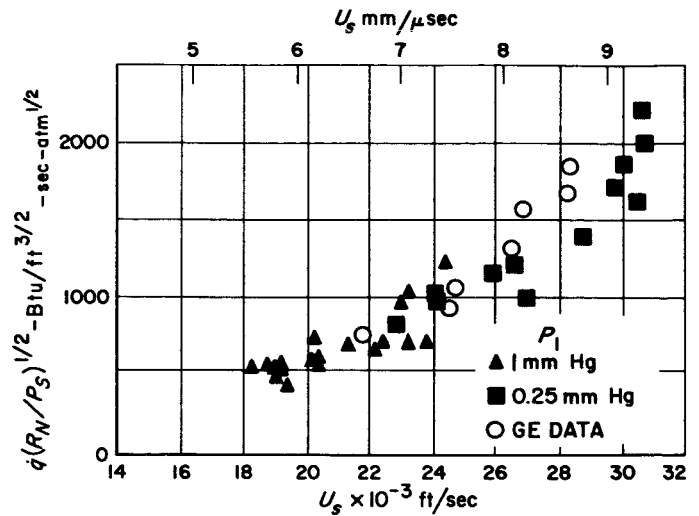


Fig. 8. Stagnation point heat transfer 9% CO₂, 90% N₂ and 1% A

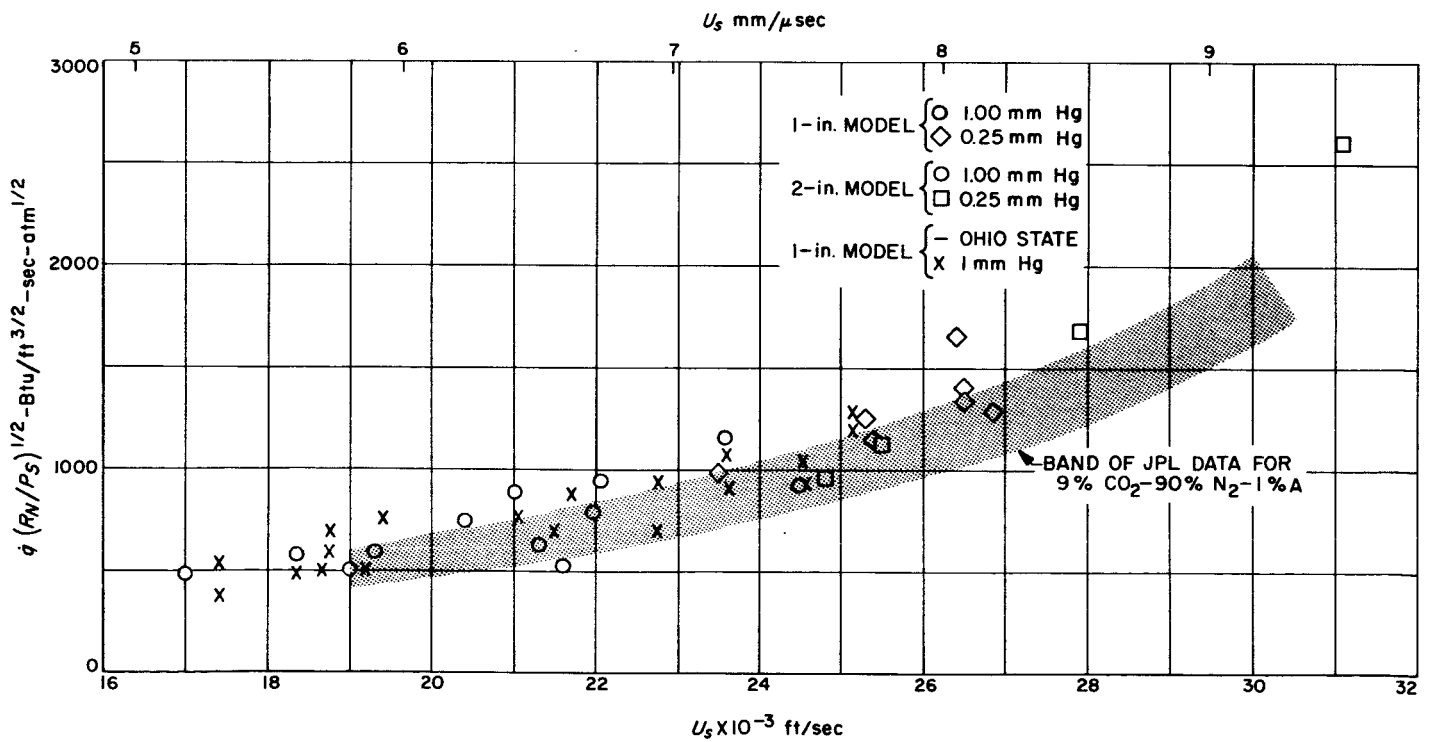


Fig. 9. Stagnation point heat transfer 100% CO₂

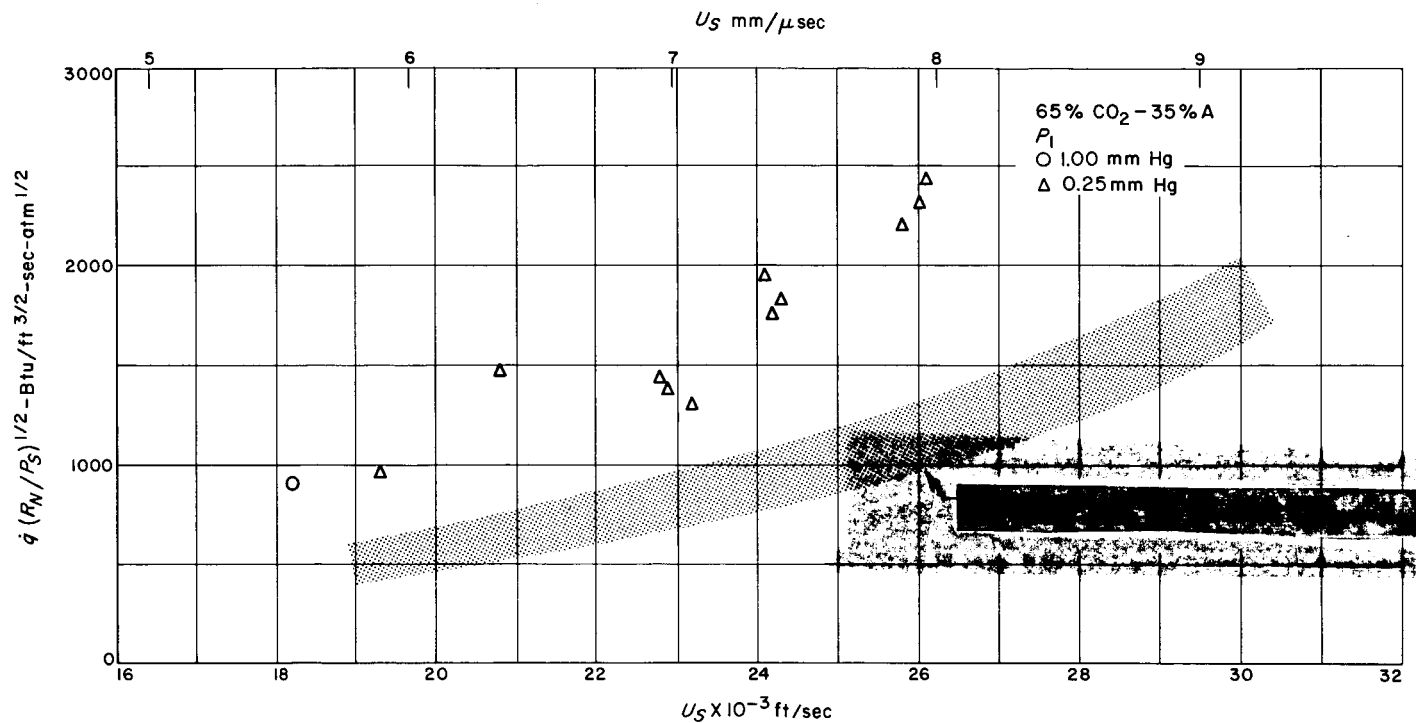
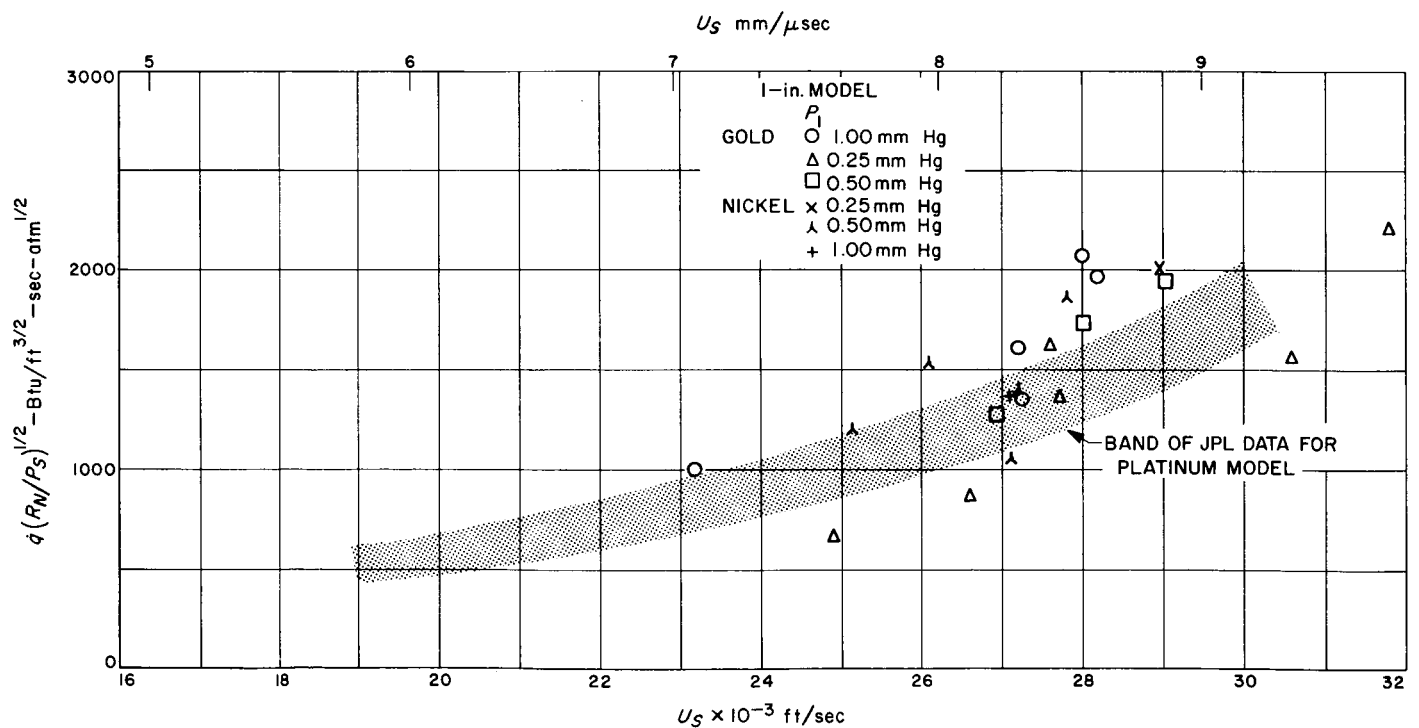
Fig. 10. Stagnation point heat transfer 65% CO₂ and 35% A

Fig. 11. Effect of different gauge materials on stagnation point heat transfer

IV. CONCLUSIONS

Convective heat transfer rates in planetary atmospheres composed of CO_2 and N_2 do not differ greatly from that of air.

The presence of argon in the atmosphere greatly increases the convective heat transfer rate.

Different calorimeter gauge materials give essentially the same heat transfer rates for the conditions investigated.

NOMENCLATURE

c	heat capacity
E	voltage
l	thickness
\dot{q}	heat transfer rate/unit area
R_o	reference resistance
t	time
α	temperature coefficient of resistance
ρ	density

REFERENCES

1. Kaplan, Lewis D., "An Analysis of the Spectrum of Mars," *The Astrophysical Journal*, Vol. 139, No. 1, January 1, 1964.
2. Collins, D. J., Livingston, F., Babineaux, T., and Morgan, N., *Hypervelocity Shock Tube*, Technical Report No. 32-620, Jet Propulsion Laboratory, Pasadena, California, June 15, 1964.
3. Rose, P. H., "Development of the Calorimeter Heat Transfer Gauge for Use in Shock Tubes," *Review of Scientific Instruments*, Vol. 29, pp. 557-564, July 1958.
4. Rose, P. H., and Stankevics, J. O., "Stagnation Point Heat Transfer Measurements in Partially Ionized Air," *AIAA Journal*, December 1963.
5. Gruszcznski, J. S., and Warren, W. R., "Experimental Heat Transfer Studies of Hypervelocity Flight in Planetary Atmospheres," *AIAA Preprint*, 63-450, August 1963.
6. Nerem, R. M., Morgan, C. J., and Graber, B. D., "Hypervelocity Stagnation Point Heat Transfer in a Carbon Dioxide Atmosphere," *AIAA Journal*, p. 2173, September 1963.
7. Collins, D. J., and Spiegel, J. M., "Effect of Gauge Materials on Convective Heat Transfer Measurements," *AIAA Journal*, p. 777, April 1964.